

CO and hydrogen adsorption on Pd(210)

Markus Lischka, Christian Mosch, and Axel Groß

Physik-Department T30, Technische Universität München, D-85747 Garching, Germany

(Dated: June 23, 2004)

We have studied the adsorption of CO on Pd(210) by performing density functional theory (DFT) calculations within the generalized gradient approximation. We find a relatively small corrugation in the CO adsorption energies with the two bridge sites being energetically almost degenerate. CO is furthermore known as a strong poison in heterogeneous catalysis. We have therefore also addressed the coadsorption of CO with atomic hydrogen. There is a significant inhibition of the hydrogen adsorption due to the presence of CO which is analysed in terms of the electronic structure of the adsorbate system.

PACS numbers: 68.35.Ja, 82.20.Kh, 82.65.Pa

Keywords: density functional calculations, chemisorption, stepped single crystal surfaces, hydrogen, carbon monoxide, palladium

I. INTRODUCTION

In the field of surface science, the study of the interaction of molecules with metal surfaces has traditionally focused on low-index surface planes. The experimental preparation of these well-defined surface in ultra-high vacuum (UHV) chambers and the subsequent adsorption of molecules on them has been a remarkable success over the past decades [1]. On the other hand, however, the surfaces of all technologically relevant catalysts are in fact non-ideal, i.e. defect-rich. Furthermore, catalytic reactions typically occur under high pressures. These discrepancies between real-world applications and basic research are called the “structure and pressure gap”.

It is a widely known fact that imperfections of the surface and coadsorbates can significantly influence the reactivity of a catalyst surface. One way to bridge the structure and pressure gap between surface science and applied heterogeneous catalysis is to carry out experimental and theoretical studies of coadsorbate systems on well-defined structured surfaces, such as vicinal surfaces of the low-index surface planes, and thus identify the effect of a particular defect structure and coadsorbate on the surface reactivity [2].

In order to contribute to the microscopic understanding of the molecular adsorption on structured surfaces, we have studied the adsorption of CO and the coadsorption of CO and hydrogen on the already rather open Pd(210) surface by density-functional theory calculations. The adsorption of carbon monoxide, CO, is one of the “prototype” systems for the study of adsorption on metal surfaces. Technologically, CO is known as a rather unwanted catalytic poison—it binds rather strongly ($\approx 1 - 2$ eV) to the surface and is able to passivate an otherwise reactive surface [3]. However, coadsorption studies are not only of interest in the context of the poisoning of a catalyst. In general, any heterogeneously catalyzed reaction requires the coadsorption of the reactants. This demonstrates the importance of a fundamental insight into the interaction between two adsorbed species.

As far as the interaction of CO with metal surfaces

is concerned, the binding to the surface is rather weak compared to the CO dissociation energy of 11.23 eV. This leads to the plausible assumption that the electronic structure of the free CO molecule is only slightly modified upon adsorption. The simple interaction picture proposed by Blyholder is capable of explaining the CO adsorption qualitatively [4–6]: Charge donation from the 5σ orbital to the metal and back donation to the $2\pi^*$ orbital establishes a metal-CO bond, but at the same time weakens the carbon-oxygen bond. Variations in the stretching frequencies of adsorbed CO can thus be explained.

Molecular CO is known for its ability to populate different adsorption sites with a very local binding, and quite a few theoretical and experimental studies on CO adsorption on different palladium surfaces exist [5, 7–21]. The (210) surface can be thought of as being built up of small (100) terraces with steps running along the [001] direction and forming open (110)-like microfacets. For atomic hydrogen, we found recently that the adsorption at the steps is energetically most favorable [22, 23]. Interestingly, according to our present study the CO adsorption on Pd(210) is not dominated by steps. CO is known to adsorb upright in bridge positions on Pd(100) [8, 11]. On Pd(210), there are two inequivalent bridge positions. And indeed, we find a relatively small corrugation in the CO adsorption energies with the two bridge sites being energetically almost degenerate.

Hydrogen on palladium has served as another prototype system for the interaction of atoms and molecules with surfaces [24–35]. A recent combined experimental and theoretical study demonstrated that on Pd(210) hydrogen can adsorb both dissociatively and molecularly [22]. These findings were rather surprising since usually H_2 adsorbs dissociatively on metal surfaces [24]. In fact, on clean Pd(210) there is no H_2 molecular adsorption state. This state becomes stabilized only if atomic hydrogen is present on the Pd(210) surface and hinders the H_2 dissociation [22, 23].

Our calculations show that CO indeed inhibits hydrogen adsorption by reducing the hydrogen adsorption en-

ergies significantly. Besides a direct electrostatic dipole-dipole repulsion, mainly the CO-induced downshift of the local d -band center is the origin for the reduction in the adsorption energies.

This paper is structured as follows. After this introduction, the computational details of our DFT study will be briefly addressed. Then we discuss the CO adsorption on the clean Pd(210) surface for CO coverages of $\theta = 1$ and $\theta = 1.5$. Finally, we address the coadsorption of CO and atomic hydrogen and finish the paper with some concluding remarks.

II. COMPUTATIONAL DETAILS

Ab initio density-functional theory calculations were used to determine all the structural, electronic and energetic results presented in this article. The Kohn-Sham equations were solved in a plane-wave basis set using the Vienna *ab initio* simulation package (VASP) [36, 37] and employing the generalized gradient approximation (GGA) of Perdew and co-workers (PW91) [38]. For an accurate representation of the oxygen core region, PAW pseudopotentials [39, 40] together with an energy cutoff of 400 eV were used. To model the surface, the slab supercell approach with periodic boundary conditions was used: The Pd(210) surface is described by periodic slabs of 11 layers and a separating vacuum region of 11 Å.

For a (1×1) surface unit cell of Pd(210), it turns out that a Monkhorst-Pack \mathbf{k} point set [41] of $7 \times 7 \times 1$, corresponding to 16 \mathbf{k} points in the irreducible Brillouin zone, together with a first-order Methfessel-Paxton smearing [42] of width $\sigma = 0.1$ eV is sufficient in order to get converged energies [23]. All reported total energies were then extrapolated to $\sigma \rightarrow 0$ eV. However, in order to find energy minimum structures it is important that also the forces are well-converged. For the clean and hydrogen-covered Pd(210) surface we have carried out relaxation calculations with a conjugate-gradient minimization scheme using the Hellman-Feynman forces computed at a larger \mathbf{k} point set of $11 \times 11 \times 1$ (36 \mathbf{k} points in the irreducible zone) [23], but we did not find any significant differences with respect to the calculation for $7 \times 7 \times 1$ \mathbf{k} points. Hence the relaxed CO adsorption structures are determined with the smaller \mathbf{k} point set.

III. RESULTS AND DISCUSSION

The properties for the CO molecule as obtained by *ab initio* DFT calculations are summarized in Table I and compared to their experimental values. All molecular properties were computed using a large, asymmetric supercell of dimensions $10.00 \times 10.25 \times 10.50$ Å. In the case of, e.g., H_2 , the asymmetry of the supercell and thus the breaking of any inherent symmetry in the atom or molecule is not important, but for molecules involving atoms with degenerate orbitals such as oxygen, the ef-

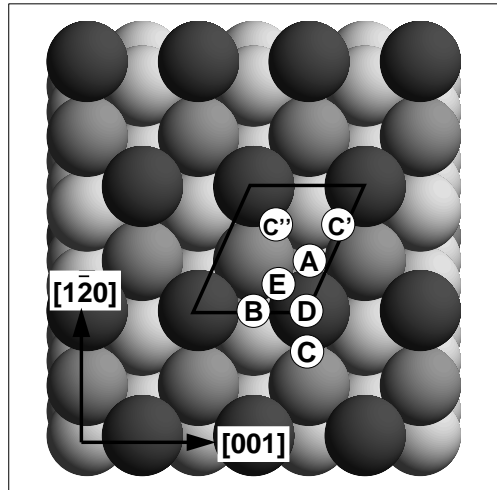


FIG. 1: Top view of the (210) surface together with the surface unit cell and CO and H adsorption sites.

fect of the supercell symmetry on the computed binding energy can become quite significant [44].

A. CO adsorption on clean Pd(210)

No evidence for any reconstruction upon CO adsorption exists experimentally [8], so that the relaxed (210) layer geometry as given in Ref. [23] was used. Since CO induced layer relaxations might be quite substantial, adsorption energies for both a slab fixed at the positions of the clean (210) surface and a fully relaxed slab are reported.

Possible CO adsorption sites are shown in Fig. 1. As CO is known to occupy bridge sites on Pd(100) or near-bridge sites on Pd(110), it is expected that sites C and E are going to be preferred adsorption sites: Site E corresponds to a bridge position on the (100) terrace, site C to a bridge position on a (110) facet. The DFT results are summarized in Table II. The obtained adsorption energies confirm this assumption: The two bridge sites E and C are the most favorable adsorption sites. They are energetically almost degenerate with adsorption energies of 1.88 eV and 1.86 eV, respectively. The effect

TABLE I: Binding energy, bond length, and stretching frequency for the CO molecule. Experimental data is taken from Ref. [43].

	CO		
	E_b [eV]	d [Å]	ω [cm^{-1}]
GGA-PAW	11.78	1.14	2135
Exp.	11.24	1.13	2170

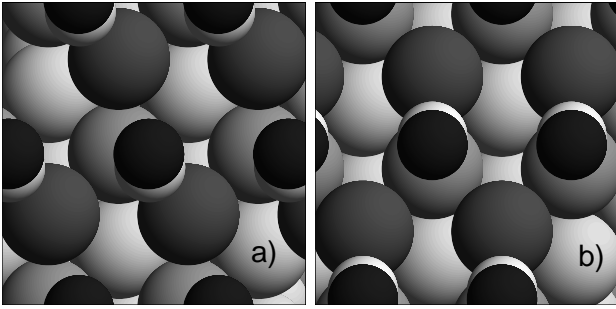


FIG. 2: Adsorption geometries for CO on Pd(210). O is drawn in black, C in white, the Pd atoms are shaded in gray. The left panel (a) illustrates the final adsorption geometry of CO at site E, the right panel (b) at site C. In both cases, the bridge-bonded, inclined CO geometry is clearly visible.

of the surface relaxation on the CO adsorption energies is relatively weak, however, it is twice as large for the C site than for the E site. It is interesting to note that CO adsorption on Pd(210) is not dominated by the step sites B; instead, there is a relatively small corrugation in the CO adsorption energies across the surface unit cell.

Adsorption at site E might be interpreted as an adsorption on a (100) terrace with an angle of 26.6° against the (210) surface, adsorption at site C as an adsorption on a (110) facet with an angle of 18.4° against the surface. Both sites are however identical as far as the direct bonding partners of the CO molecule are concerned, only the next-nearest neighbors are different. Relaxed adsorption geometries for both sites are detailed in Table III, and the computed atom distances are identical within our numerical accuracy. Furthermore, the CO molecule is bonding almost perpendicular to the line connecting its two respective, fully relaxed palladium partners and perfectly centered in its bridge position in both cases: We only note one Pd-C distance in Table III as differences are below 0.005 \AA . However, the induced layer relaxations at site C are much stronger than at site E,

TABLE II: Adsorption energies per molecule for different adsorption sites of CO on Pd(210). The notation of the sites refers to Fig. 1. For adsorption at the on-top site, the molecule was laterally constrained to position D.

Coverage	Site	E_{ad} [eV]		
		Fixed slab	Relaxed slab	Exp.[45]
$\theta = 1$	E	1.83	1.88	1.45
	C	1.76	1.86	
	B	1.73	1.77	
	A	1.50	1.58	
$\theta = 1.5$	D	1.48	1.50	
		0.91	—	1.14

changing the orientation of the Pd-Pd axis between first and second layer and thus allowing the molecule to position itself in a more upright fashion while still perfectly preserving its bridge-bonding position. This also explains the relatively large energy gain at this position when relaxing the substrate. In particular, there is a surprisingly strong outward relaxation between the second and third layer. Note that at the clean surface, DFT calculations yield a reduction of d_{23} with respect to the bulk value of -3% [23].

Experimentally, electron stimulated desorption ion angular distribution (ESDIAD) measurements [9] at low coverages up to $\theta = 1$ suggest adsorption of CO in a bridge-bonded position at site E, inclined away from the surface normal, in agreement with our DFT results. Thermal desorption results yield an initial adsorption energy of 1.52 eV [7] or 1.45 eV per molecule [45]. The binding energy for the bridge site E is thus considerably overestimated. GGA calculations using the PW91 exchange-correlation functional, however, tend to overestimate the CO adsorption on a wide range of metal surfaces [46].

For the CO adsorption on Pd(100), we obtain an adsorption energy of 1.91 eV at the bridge position for the $c(2\sqrt{2} \times \sqrt{2})$ CO superstructure, in good agreement with previous calculations using a slightly different setup [11]. Note that the $c(2\sqrt{2} \times \sqrt{2})(100)$ and the $(1 \times 1)(210)$ surface unit cells have approximately the same area so that these calculations correspond to comparable coverages. Nevertheless, it is surprising that the adsorption energy of CO in fact turns out to be slightly lower on Pd(210) than on Pd(100). Given the low coordination of the top Pd atom and thus its high reactivity, it might be anticipated that CO is actually strongly bound to Pd(210). For on-top adsorption, this is indeed true: Adsorption at site D gives a binding energy of 1.50 eV , whereas on-top adsorp-

TABLE III: Adsorption geometries for CO on Pd(210) at a coverage of $\theta = 1$. The used notation for the bonding lengths and angle is illustrated in the figure. For the interlayer spacings, d_{12} and d_{23} , the relative change in % to the bulk value is given in parentheses. Note that, on a fixed slab, CO adsorption in a bridge-bonded, locally perpendicular orientation at site C corresponds to an inclination of $\theta_{\text{C-O}} = 18.4^\circ$ as measured against the surface normal.

Site	$d_{\text{Pd-C}}$ [Å]	$d_{\text{C-O}}$ [Å]	$\theta_{\text{C-O}}$ [°]	d_{12} [Å]	d_{23} [Å]
E	1.99	1.18	18.0	0.760 (-14)	0.950 (+7)
C	1.99	1.18	12.0	0.723 (-18)	1.023 (+15)

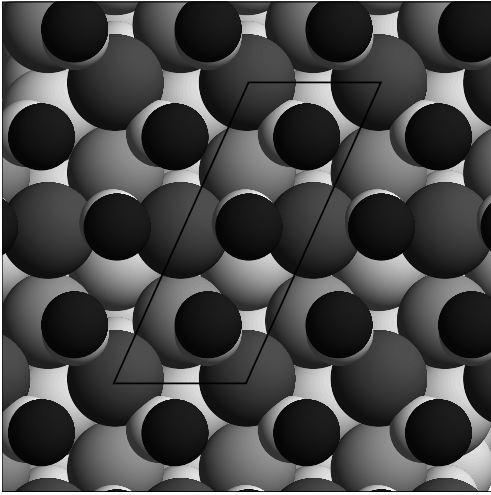


FIG. 3: Adsorption geometry of CO/Pd(210) at a coverage of $\theta = 1.5$. The color coding is identical to the one used in Fig. 2. The CO molecules are (approximately) located at sites E, B, and C' (from bottom to top). The (1×2) surface unit cell is also shown.

tion on Pd(100) gives 1.44 eV [11]. As in both cases the nearest-neighbor distance of the CO molecules is identical, i.e., the Pd lattice constant, a_0 , any dipole-dipole repulsion effects should be comparable and thus not change any relative differences. Besides, dipole-dipole interactions at a similar coverage on Pd(110) were estimated to be on the order of 30 meV [17]. Experimental TDS results, too, suggest a slightly higher adsorption energy on Pd(100) than on Pd(210) [7]. As seen in Table III, adsorption in both bridge-bonded sites results in rather strong relaxations, and a tendency to minimize the CO inclination is always found. This suggests that the CO molecule is just repelled by the protruding Pd atom at the next “step”, and adsorption is thus not as favorable as on a flat (100) surface. Furthermore, variations in the CO adsorption energy from site to site are comparably small and a rather small energy gain due to a more reactive bonding partner might just be overcompensated by the enforced, but unfavorable inclination of the molecule.

On Pd(110), CO adsorbs in a near-bridge site at monolayer coverage. The molecules are alternately tilted along the [100] direction (perpendicular to the top layer rows), resulting in a (2×1) periodicity [15] forming a “zig-zag” chain of CO molecules. In contrast to the situation on the (210) surface, each Pd atom binds two alternately tilted CO molecules. Computations in a (1×2) unit cell of the (210) surface revealed no evidence for such an alternating structure on the (210) surface.

The experimental saturation coverage of CO on Pd(210) is reported to be $\theta = 1.5$ [7]. LEED experiments show that this coverage is achieved by maintaining rows of CO molecules along the [001] direction, but reducing the CO distances along the $[1\bar{2}0]$ direction. A possible microscopic structure is shown in Fig. 3. The energy gain

of additional adsorption of one CO molecule per (1×2) unit cell going from $\theta = 1.0$ to $\theta = 1.5$ is 0.91 eV. The CO molecules rearrange in such a way that one of them stays in the most favorable E site, whereas the other two rows of CO molecules are pushed to approximately the B and C' sites. In comparison, TDS results yield a weaker bound β_1 species with an adsorption energy of 1.14 eV [45]. It is in fact surprising that the differential heat of adsorption for a coverage of $\theta = 1.5$ seems to be underestimated while it is overestimated at low coverages. However, no comprehensive scan of possible structures in the (1×2) unit cell was performed so that the existence of other structures lower in energy cannot be ruled out.

Corresponding to the large intrinsic dipole moment of the CO molecule, a CO coverage of $\theta = 1.5$ results in a significant work function increase of $\Delta\Phi = 1.45$ eV ($\Phi = 6.37$ eV). At a coverage of $\theta = 1.0$, a still considerable increase of 1.26 eV is found ($\Phi = 6.18$ eV). In CO adsorption experiments on Pd(210), a maximum increase of the work function by 1.06 eV is reported [7]. Similar to hydrogen-induced work function changes [22], the computed effect of the adsorbate on the work function is thus overestimated.

CO bonding to a metal surface is usually discussed in terms of the Blyholder model [4]. A more thorough discussion can be based on the analysis of the resulting mixed orbitals as they are manifested in the respective local density of states [47, 48]. In Fig. 4, the local density of states for both the top Pd atom and the carbon and oxygen atoms are depicted. The d -band centers were determined by integration over the available energy range fully including all d -band states. Upon CO adsorption, the Pd d -band center is shifted down from -1.26 eV to -1.82 eV. The CO 1π , $2\pi^*$ and the Pd d orbitals with π symmetry hybridize to give an all-bonding $1\tilde{\pi}$, a non-bonding \tilde{d}_π , and an anti-bonding $2\tilde{\pi}^*$ orbital [47]. On the other hand, the CO 4σ , 5σ and the Pd d_σ interact to form bonding $4\tilde{\sigma}$ and $5\tilde{\sigma}$ orbitals as well as a broad anti-bonding \tilde{d}_σ band. In Fig. 4, the broad resonance of the CO orbitals with the respective metal d -band orbitals in the energy range of -5 to 0 eV are clearly visible. The much lower density of states in this region at the carbon atom can be traced back to the non-bonding character of the \tilde{d}_π orbital, with its reduced charge density at the carbon atom due to its nodal plane there. As expected, the distance between the modified 4σ ($E = -9.5$ eV) and 5σ orbitals ($E = -6.7$ eV) is significantly reduced, and the 5σ orbital is even located below the 1π -deduced states ($E = -6.5$ eV and $E = -6.0$ eV) in contrast to the free CO molecule. The derived bonding scenario is very similar to the one found for bridge site adsorption of CO on Pd(100) [11]. We also note that at different adsorption sites there are subtle differences as far as the importance of the hybridization of the metal d states with the 5σ and the $2\pi^*$ orbitals of CO is concerned [11, 49]. It is thus well conceivable that the upshift of the d -band center at the open Pd(210) surface [23] has opposing effects on the bonding mechanisms at the top and bridge sites leading

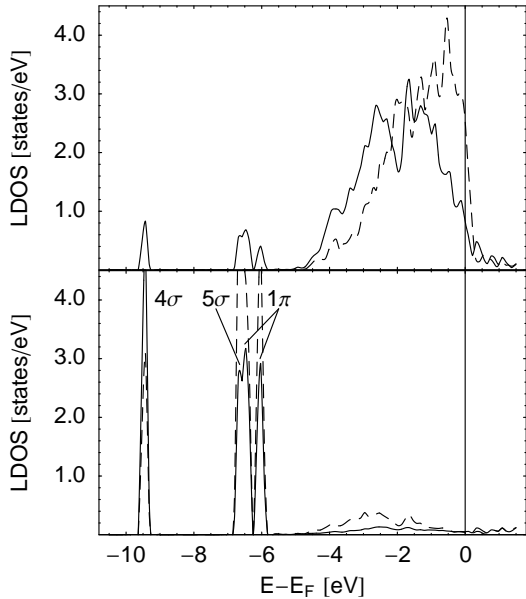


FIG. 4: LDOS analysis of CO adsorbed at the bridge site E on Pd(210). Upper panel: Local d -band density of states of the top-most Pd atom before (dashed) and after (solid) CO adsorption. The d -band center is shifted from -1.26 eV to -1.82 eV upon CO adsorption. Lower panel: Local DOS (summed over all orbitals) at the carbon (solid) and oxygen atom (dashed) with a projection radius of $r = 1.058$ Å (2 bohr). The resonant levels are labeled according to the orbitals they originate from in the free gas-phase CO molecule as revealed by an analysis of the orbital-resolved DOS. The peak at -6.6 eV exhibits a double-peak structure with both 5σ and 1π contributions.

to the reduced corrugation in the adsorption energies.

This interaction picture is also capable of accounting for the fact that CO always adsorbs with the carbon atom towards the surface [47]. On Pd(210), DFT calculations with the oxygen pointing towards the surface gives a roughly non-bonding scenario yielding no net energy gain in contrast to the large adsorption energy of 1.88 eV for carbon-terminated bonding. In the described final electronic structure after the metal d -band interaction is taken into account, both the interactions of the σ and the π orbitals result in a net charge transfer to the atom not bonding to the surface. As the oxygen atom is more electronegative, adsorption with the carbon atom towards the surface yields a much larger adsorption energy. In addition, the 5σ orbital is mainly located at the carbon atom [5, 11, 12] which leads to a larger overlap with the Pd surface for the carbon end down and thus to a stronger interaction compared to the situation with the oxygen atom down.

B. Coadsorption of H and CO on Pd(210)

The adsorption energies of CO on Pd(210) are significantly larger than those of hydrogen on Pd(210). It is thus very likely that any coadsorption of carbon monoxide and hydrogen will be dominated by the CO molecule. Nevertheless, due to the rather open structure of the (210) surface, atomic or even molecular hydrogen adsorption might still be possible. On a specially prepared Ni(100) surface covered with hydrogen and carbon monoxide, for instance, a structural transformation upon heating and the formation of chemisorbed H_2 is found [50]. However, coadsorption experiments of CO and H_2 showed a strong inhibition of hydrogen adsorption [45].

The computed atomic hydrogen adsorption energies for one hydrogen atom per surface unit cell in the presence of CO at different sites are listed in Table IV. In addition, the atomic hydrogen adsorption energies on clean Pd(210) are included as a reference [23]. The atomic H adsorption energies were computed with respect to the theoretical binding energy of H_2 in the PAW pseudopotential approximation. Note that the bridge site C is no stable atomic hydrogen adsorption site, the H atom rather relaxes towards the quasi-threefold C' site.

The overall trend is a significant reduction of atomic hydrogen adsorption energies at all sites due to the presence of CO on Pd(210), in agreement with the experi-

TABLE IV: Atomic hydrogen adsorption energies in eV/atom on clean [23] and CO precovered Pd(210). The coverage corresponds to one H atom and one CO molecule per (210) surface unit cell. If the adsorption site is not stable, the relaxation path of the adsorbate is indicated.

CO-pos	H-pos	E_{ad} (eV)	
		Fixed slab	Relaxed slab
–	A	–	0.45
–	B	–	0.52
–	C ^(*)	–	0.44
–	C'	–	0.51
E	A	0.09	0.12
E	C'	0.22	0.31
E	C''	0.19	0.27
E	B	H-pos: B → C'	H-pos: B → C'
C	A	0.13	0.22
C	B	0.24	0.30
C	C''	H-pos: C'' → B	H-pos: C'' → B
C	E	H-pos: E → B	H-pos: E → B
B	A	0.16	0.22
B	C	0.04	0.08
B	C''	CO-pos: B → E	CO-pos: B → E
B	E	H-pos: E → A	H-pos: E → A

(*) This site is not stable for hydrogen adsorption (see text)

mental results [45]. For CO adsorbed on the energetically most favorable site E, the threefold coordinated site C' is the only one to remain somewhat reactive with respect to hydrogen adsorption. Due to the adsorbed CO molecule, the mirror symmetry along $[1\bar{2}0]$ and thus the degeneracy of sites C' and C'' is removed: The adsorption energy at site C'' is slightly reduced in comparison to site C' as the distance of the hydrogen atom to the neighboring CO molecules is shorter. A hydrogen atom experiences an even larger repulsion at site A since it is rather close to the adsorbed CO molecule. At the step site B, the most reactive one on the clean (210) surface, atomic hydrogen is no longer stable as the hydrogen is pushed to the neighboring C' site instead. This can be understood by looking at the dissociation of formyl, HCO, on a metal surface [51]. Once the carbon-bonded hydrogen (starting from a gas-phase bond length of approximately 1.1 Å) is slightly separated from the carbon atom, both being in contact with the metal surface, the hydrogen is strongly repelled and separates itself from the remaining CO. In this context, it is clear that the hydrogen molecule tries to maximize its distance to all neighboring CO molecules.

Site C is energetically almost degenerate with site E with regard to the CO adsorption. According to Table IV, the CO induced reduction in the hydrogen binding energies is also similar. At site A, the hydrogen adsorption energy is less affected by CO on site C than on site E because of the larger CO-H distance. Hydrogen placed both on site C'' and on site E is unstable and pushed to site B. Note that hydrogen usually prefers high-coordinated sites on Pd surfaces and that therefore the bridge site E is also an unstable hydrogen adsorption site on clean Pd(210).

Finally we address the coadsorption of CO and H for CO located at the step site B. For this configuration, hydrogen can only adsorb on site A with an appreciable binding energy. Site C is no longer unstable for H adsorption as on the clean surface due to the repulsion caused by the CO molecules which are located symmetrically at both adjacent B sites. However, this repulsion also leads to a significant lowering of the atomic hydrogen adsorption energies. Interestingly, for hydrogen located at site C'', the CO adsorption site B is no longer metastable, i.e. no local energy minimum. Now it is not the hydrogen atom that is displaced upon energy minimisation, but rather the CO molecule that is shifted towards its most favorable adsorption site E. This is a consequence of the relatively small corrugation of the CO adsorption energies on Pd(210). An H atom placed on site E is again unstable and rather adsorbs on site A.

With respect to the mechanism of the poisoning of the hydrogen adsorption by preadsorbed CO on Pd(210), we note that both atomic hydrogen and CO lead to an increase of the work function upon adsorption. Thus they should experience a mutual dipole-dipole repulsion when they are coadsorbed. In the discussion above, we have seen that the reduction in the hydrogen adsorption energies caused by the presence of CO correlates with the

CO-H distance which is indicative of a direct repulsive interaction.

However, the increase of the work function upon atomic hydrogen adsorption is rather small, about 0.2 eV [22]. Besides, we note that atomic hydrogen is adsorbed much closer to the surface than CO. At site B, the hydrogen atom is located at about the same height as the uppermost Pd layer while at the other hydrogen adsorption sites (A, C' and C'') it is even 0.2 – 0.8 Å below the uppermost Pd layer. In contrast, the center of mass of the adsorbed CO molecule is located about 2 Å above the top Pd layer. Thus the influence of the dipole-dipole interaction on the hydrogen adsorption energies should be limited. As far as the coadsorption of CO with water on Pd/Au overlayers is concerned, also a relatively weak dipole-dipole interaction between CO and H₂O has been found in recent DFT calculations [52].

Apart from the direct interaction between the coadsorbates, the CO-induced modification of the substrate density of states can also lead to significant changes in the hydrogen adsorption energies. This indirect substrate-mediated mechanism has for example been discussed in the case of the poisoning of hydrogen dissociation at Pd(100) by adsorbed sulfur [53, 54]. The change in the adsorption energies can be understood in terms of the *d*-band model [55]. According to the *d*-band model, an energetic downshift of the position of the local *d*-band center leads to smaller chemical binding at the particular surface. Analogously to the situation of a Pd(210) surface pre-covered with hydrogen [23], the *d*-band center is reduced with respect to its value on the clean surface upon CO adsorption. The *d*-band center of the top Pd atom shifts from $\varepsilon_d = -1.26$ eV to $\varepsilon_d = -1.82$ eV. Due to the significant interaction of the CO molecule with its neighboring Pd atoms, this shift is much larger than in the case of a monolayer of atomic hydrogen. This strong down-shift thus explains the rather large decrease in the hydrogen binding energies on the CO-covered surface.

On clean Pd(210), a coexistence of atomic and molecular hydrogen adsorption states has been found [22]. DFT calculations have demonstrated that atomic hydrogen at site B hinders the dissociation of additional H₂ above the top Pd atom (site D, see Fig. 1). Thus the H₂ molecular adsorption state becomes metastable with a binding energy of 0.27 eV per H₂ molecule. On the CO precovered surface, H₂ molecular adsorption is no longer exothermic. For CO adsorbed at site E, the H₂ adsorption energy at the top Pd atom is now even slightly negative (−0.01 eV per H₂ molecule) with respect to the gas phase H₂ energy, although it is still a metastable site separated by a barrier from the vacuum. Note that the H₂ adsorption on hydrogen covered Pd(210) leads to a decrease of the work function; hence there should be an attractive dipole-dipole interaction between adsorbed H₂ and CO. The fact that H₂ molecular adsorption is no longer exothermic on CO-covered Pd(210) confirms that it is predominantly the CO-induced downshift of the local Pd *d*-band center which is responsible for the reduction of

the hydrogen adsorption energies.

IV. CONCLUSIONS

We have performed density functional theory calculations to study the adsorption of CO and the coadsorption of CO and hydrogen on the (210) surface of palladium. We found that the variation of the CO binding energy is comparably small across different adsorption sites and that bonding of CO is a very local process. As on the Pd(100) surface, CO prefers to adsorb in a bridge configuration on Pd(210) with the two inequivalent bridge sites being energetically practically degenerate. At the bridge site on the (100) terrace, CO adsorbs inclined with respect to the surface normal. An analysis of the LDOS yielded a very similar picture to the one found

on a flat (100) surface. Atomic adsorption energies on a CO-precovered surface are significantly reduced, and molecular H₂ adsorption becomes completely inhibited in contrast to the H-precovered Pd(210) surface. Apart from direct electrostatic repulsion, the poisoning effect of CO is a consequence of the strong modification of the Pd *d*-band upon CO adsorption.

Acknowledgments

Financial support by the Deutsche Forschungsgemeinschaft through project GR 1503/11-1 is gratefully acknowledged. We also thank P. K. Schmidt and K. Christmann (Freie Universität Berlin) for sharing their results with us prior to publication and for many useful discussions.

-
- [1] C. B. Duke, editor, *Surface Science: The first thirty years*, volume 299/300 of *Surf. Sci.*, 1994.
- [2] A. Groß, *Surf. Sci.* **500** (2002) 347.
- [3] E. Christoffersen, P. Liu, A. Ruban, H. L. Skriver, and J. K. Nørskov, *J. Catal.* **199** (2001) 123.
- [4] G. Blyholder, *J. Phys. Chem.* **68** (1964) 2772.
- [5] P. Hu, D. A. King, M.-H. Lee, and M. C. Payne, *Chem. Phys. Lett.* **246** (1995) 73.
- [6] H. Aizawa and S. Tsuneyuki, *Surf. Sci.* **399** (1998) L364.
- [7] H. Conrad, G. Ertl, J. Koch, and E. E. Latta, *Surf. Sci.* **43** (1974) 462.
- [8] A. M. Bradshaw and F. M. Hoffmann, *Surf. Sci.* **72** (1978) 513.
- [9] T. E. Madey, J. T. Yates, Jr., A. M. Bradshaw, and F. M. Hoffmann, *Surf. Sci.* **89** (1979) 370.
- [10] R. J. Behm, K. Christmann, G. Ertl, and M. A. Van Hove, *J. Chem. Phys.* **73** (1980) 2984.
- [11] A. Eichler and J. Hafner, *Phys. Rev. B* **57** (1998) 10110.
- [12] F. Delbecq and P. Sautet, *Phys. Rev. B* **59** (1999) 5142.
- [13] K. Honkala, P. Pirilä, and K. Laasonen, *Surf. Sci.* **489** (2001) 72.
- [14] M. K. Rose, T. Mitsui, J. Dunphy, A. Borg, D. F. Ogletree, M. Salmeron, and P. Sautet, *Surf. Sci.* **512** (2002) 48.
- [15] M. Kittel, R. Terborg, M. Polcik, A. M. Bradshaw, R. L. Toomes, D. P. Woodruff, and E. Rotenberg, *Surf. Sci.* **511** (2002) 34.
- [16] M. Hirsimäki and M. Valden, *J. Chem. Phys.* **114** (2001) 2345.
- [17] H. S. Kato, H. Okuyama, J. Yoshinubo, and M. Kawai, *Surf. Sci.* **513** (2002) 239.
- [18] R. D. Ramsier, K.-W. Lee, and J. T. Yates, Jr., *Surf. Sci.* **322** (1995) 243.
- [19] S. Katsuki and H. Taketa, *Solid State Comm.* **39** (1981) 711.
- [20] A. Roudgar and A. Groß, *Phys. Rev. B* **67** (2003) 033409.
- [21] A. Roudgar and A. Groß, *J. Electronal. Chem.* **548** (2003) 121.
- [22] P. K. Schmidt, K. Christmann, G. Kresse, J. Hafner, M. Lischka, and A. Groß, *Phys. Rev. Lett.* **87** (2001) 096103.
- [23] M. Lischka and A. Groß, *Phys. Rev. B* **65** (2002) 075420.
- [24] K. Christmann, *Surf. Sci. Rep.* **9** (1988) 1.
- [25] K. D. Rendulic, G. Anger, and A. Winkler, *Surf. Sci.* **208** (1989) 404.
- [26] K. D. Rendulic and A. Winkler, *Surf. Sci.* **299/300** (1994) 261.
- [27] A. Groß, S. Wilke, and M. Scheffler, *Phys. Rev. Lett.* **75** (1995) 2718.
- [28] S. Wilke and M. Scheffler, *Phys. Rev. B* **53** (1996) 4926.
- [29] A. Groß, *Appl. Phys. A* **67** (1998) 627.
- [30] W. Dong, V. Ledentu, P. Sautet, A. Eichler, and J. Hafner, *Surf. Sci.* **411** (1998) 123.
- [31] C. Crespos, H. F. Busnengo, W. Dong, and A. Salin, *J. Chem. Phys.* **114** (2001) 10954.
- [32] H. F. Busnengo, E. Pijper, M. F. Somers, G. J. Kroes, A. Salin, R. A. Olsen, D. Lemoine, and W. Dong, *Chem. Phys. Lett.* **356** (2002) 515.
- [33] M. A. Di Cesare, H. F. Busnengo, W. Dong, and A. Salin, *J. Chem. Phys.* **118** (2003) 11226.
- [34] M. Lischka and A. Groß, Hydrogen on palladium: a model system for the interaction of atoms and molecules with metal surfaces, in *Recent Developments in Vacuum Science and Technology*, edited by J. Dabrowski, pages 111–132, Research Signpost, Kerala (India), 2003.
- [35] T. Mitsui, M. K. Rose, E. Fomin, D. F. Ogletree, and M. Salmeron, *Nature* **422** (2003) 705.
- [36] G. Kresse and J. Furthmüller, *Phys. Rev. B* **54** (1996) 11169.
- [37] G. Kresse and J. Furthmüller, *Comput. Mater. Sci.* **6** (1996) 15.
- [38] J. P. Perdew, J. A. Chevary, S. H. Vosko, K. A. Jackson, M. R. Pederson, D. J. Singh, and C. Fiolhais, *Phys. Rev. B* **46** (1992) 6671.
- [39] P. E. Blöchl, *Phys. Rev. B* **50** (1994) 17953.
- [40] G. Kresse and D. Joubert, *Phys. Rev. B* **59** (1999) 1758.
- [41] H. J. Monkhorst and J. D. Pack, *Phys. Rev. B* **13** (1976) 5188.
- [42] M. Methfessel and A. T. Paxton, *Phys. Rev. B* **40** (1989) 3616.
- [43] G. Herzberg and K. P. Huber, *Molecular Spectra and Molecular Structure. IV. Constants of Diatomic*

Molecules, Van Nostrand Reinhold, 1979.

- [44] F. W. Kutzler and G. S. Painter, *Phys. Rev. Lett.* **59** (1987) 1285.
- [45] P. K. Schmidt, *Wechselwirkung von Wasserstoff mit einer Pd(210)- und Ni(210)-Oberfläche*, PhD thesis, Freie Universität Berlin, 2002.
- [46] E. Christoffersen, P. Stoltze, and J. K. Nørskov, *Surf. Sci.* **505** (2002) 200.
- [47] A. Föhlisch, M. Nyberg, P. Bennich, L. Triguero, J. Hasselström, O. Karis, L. G. M. Pettersson, and A. Nilsson, *J. Chem. Phys.* **112** (2000) 1946.
- [48] A. Föhlisch, M. Nyberg, J. Hasselström, O. Karis, L. G. M. Pettersson, and A. Nilsson, *Phys. Rev. Lett.* **85** (2000) 3309.
- [49] G. Kresse, A. Gil, and P. Sautet, *Phys. Rev. B* **68** (2003) 073401.
- [50] L. Westerlund, L. Jönsson, and S. Andersson, *Surf. Sci.* **187** (1987) L669.
- [51] J. Greeley and M. Mavrikakis, *J. Am. Chem. Soc.* **124** (2002) 7193.
- [52] A. Roudgar and A. Groß, *subm. to Surf. Sci.*
- [53] S. Wilke and M. Scheffler, *Surf. Sci.* **329** (1995) L605.
- [54] C. M. Wei, A. Groß, and M. Scheffler, *Phys. Rev. B* **57** (1998) 15572.
- [55] B. Hammer and J. K. Nørskov, *Surf. Sci.* **343** (1995) 211.